

# A Fingerprint for Large Language Models

Zhiguang Yang

School of Communication & Information  
Engineering, Shanghai University  
Shanghai 200444, China  
yangzg@shu.edu.cn

Hanzhou Wu

School of Communication & Information  
Engineering, Shanghai University  
Shanghai 200444, China  
h.wu.phd@ieee.org

**Abstract**—Recent advances show that scaling a pre-trained language model could achieve state-of-the-art performance on many downstream tasks, prompting large language models (LLMs) to become a hot research topic in the field of artificial intelligence. However, due to the resource-intensive nature of training LLMs from scratch, it is urgent and crucial to protect the intellectual property of LLMs against infringement. This has motivated the authors in this paper to propose a novel black-box fingerprinting technique for LLMs, which requires neither model training nor model fine-tuning. We first demonstrate that the outputs of LLMs span a unique vector space associated with each model. We model the problem of ownership authentication as the task of evaluating the similarity between the victim model’s space and the output’s space of the suspect model. To deal with this problem, we propose two solutions, where the first solution involves verifying whether the outputs of the suspected large model are in the same space as those of the victim model, enabling rapid identification of model infringement, and the second one reconstructs the union of the vector spaces for LLM outputs and the victim model to address situations where the victim model has undergone the Parameter-Efficient Fine-Tuning (PEFT) attacks. Experimental results indicate that the proposed technique achieves superior performance in ownership verification and robustness against PEFT attacks. This work reveals inherent characteristics of LLMs and provides a promising solution for ownership verification of LLMs in black-box scenarios, ensuring efficiency, generality and practicality.

**Index Terms**—Intellectual property protection, large language model, fingerprint, security, Transformer, deep learning.

## I. INTRODUCTION

Large Language Models (LLMs) have emerged as a cornerstone of modern artificial intelligence, exhibiting remarkable performance across various natural language processing tasks due to their capability to generate human-like texts and comprehend human language. Despite the substantial data samples and computational resources required to train LLMs, numerous developers continue to advance research by open-sourcing their models. Many organizations and researchers, including those behind well-known models such as LLaMA, Gemma and Mistral [1]–[4], have released their well-trained LLMs to the public. The thriving universe of LLMs is driven by its entirely open-source nature. However, malicious users may exploit developed LLMs for illegal purposes such as fine-tuning with another pre-trained model without attribution or stealing a model and claiming it as their own asset. Therefore, safeguarding intellectual property rights of LLMs is essential,

not solely to maintain commercial value but also to promote the sustainable development of the open-source community.

Numerous studies have employed digital watermarking and fingerprinting methods to protect deep neural network (DNN) models. Uchida *et al.* [5] first introduced a regularization term to constrain the network weights for embedding watermarks. Subsequently, scholars have proposed various methodologies to embed watermarks into the model parameters in white-box scenarios, where the extractor can access the entirety of model parameters [6]–[8]. However, the challenges in accessing all the model parameters in various scenarios has led to a focus on black-box techniques for model watermarking. Many watermarking methods utilize backdoor techniques, constructing specific input-output mappings and observing the output of the DNN model for verification [9]–[11]. Generative models, particularly image processing models, often produce contents with high entropy and sufficient information capacity to accommodate additional watermark information, which remains highly imperceptible. Wu *et al.* [12] introduced a watermark framework to make the output contents of the model contain a certain watermark. Lukas *et al.* [13] proposed embedding watermarks by fine-tuning the image generator, ensuring that all images produced are watermarked. Fernandez *et al.* [14] extended it to the diffusion model. Embedding watermarks through backdoor and fine-tuning techniques compromises the primary functionality of the model to a certain extent and requires significant computational resources. Song *et al.* [15] distinguished different generative models based on their artifacts and fingerprints, which can help alleviate this problem.

The emergence of superior reasoning capabilities in LLMs which require significant computational overhead, poses new challenges for their protection. Xu *et al.* [16] specified a confidential private key and embedded it as an instructional backdoor, serving as a fingerprint. Zeng *et al.* [17] utilized the internal parameters in Transformer [18] as a fingerprint to identify the LLMs. Existing methods typically require white-box access or fine-tuning to verify the copyright information. In contrast, our proposed fingerprinting method can be implemented in a black-box scenario without any fine-tuning.

We present a novel fingerprinting method for LLMs that analyzes the output of the LLMs for model authentication. LLMs generate semantically coherent and reasonable texts by sampling from logits, which themselves contain substantial model-related information. In black-box scenarios, LLM

Corresponding author: Hanzhou Wu (contact email: h.wu.phd@ieee.org)

providers often offer complete or partial logits vectors, enabling users to apply various sampling methods to generate realistic contents. Carlini *et al.* [19] demonstrated the ability to extract portions of a model solely through API access. We implement LLM fingerprinting from a novel perspective, identifying unique attributes of each LLM by analyzing their logits output. Previous works have shown that the output of LLMs resides in a linear subspace defined by their parameters [20]–[22]. We retain the parameters of the victim model, specifically the last linear layer. By querying the suspect model and obtaining its output, we use the retained parameters to determine the unique attribution of the suspect model. We identify ownership authentication as comparing the similarity between the victim model’s vector space and the suspect model’s output space. We initially propose a method to swiftly ascertain whether the output originates from the victim model by determining its compatibility with the vector space formed by the retained parameters. To address scenarios involving Parameter-Efficient Fine-Tuning (PEFT) attacks, we develop an alignment-verification method to determine if the suspect model was derived through PEFT by comparing similarities. Furthermore, through API access, we are able to reconstruct complete logits from partial ones to verify ownership. Our method enables ownership verification in black-box scenarios solely through API access and does not depend on the specific structure of LLMs. This ensures generalizability and provides an effective and promising approach for copyright protection of LLMs. Our experiments demonstrate that the proposed method achieves supervisor verification performance and robustness against PEFT attacks, without any compromise in model functionality.

In summary, the main contributions of this work include:

- By analyzing the characteristics of LLMs from a novel perspective, we demonstrate that their outputs can serve as fingerprints for ownership verification.
- We propose two distinct methods for implementing ownership verification of LLMs: one quickly determines whether the output originates from the victim model, and the other verifies whether the suspected model has been subjected to a PEFT attack from the victim model.
- We present a method to recover complete information for fingerprint verification by obtaining partial logits through API access.

The remainder of this paper is organized as follows: Section II provides an overview of fingerprinting, PEFT and the threat model. Section III explains the LLM fingerprinting method. In Section IV, we detail the two proposed ownership verification methods, followed by our experimental results and analysis in Section V. Finally, we conclude this paper in Section VI.

## II. PRELIMINARIES

### A. Fingerprinting

The model provider releases the model  $\mathcal{M}_\theta$ , including its complete structure and parameters. Once a model is released, it may be stolen by malicious users who may either directly steal

it or fine-tune it and claim ownership. We protect the legitimate rights of the model publisher by analyzing distinctive features found in the parameters or output of the model as fingerprints. In this study, we utilize the output of LLMs as fingerprints for model verification.

### B. Parameter-Efficient Fine-Tuning

Training or fine-tuning DNNs based on pre-training requires substantial resources, particularly for LLMs, which demand significant GPU memory. Recent research focuses on efficient fine-tuning methods that achieve optimization with fewer parameters [23]–[25]. Parameter-Efficient Fine-Tuning (PEFT) is used to fine-tune a model with minimal parameters. Low-Rank Adaptation (LoRA) [24] has become the de facto method for PEFT, serving as the foundation for many other approaches such as [25], [26]. In LoRA, the weight matrix  $\mathbf{W}_O$  is updated by the formula  $\mathbf{W}_N = \mathbf{W}_O + \Delta\mathbf{W} = \mathbf{W}_O + \mathbf{A}\mathbf{B}$ . During training,  $\mathbf{W}_O$  remains fixed, while the two matrices  $\mathbf{A}$  and  $\mathbf{B}$  encompass the least trainable parameters. This study uses LoRA to mimic the PEFT attack.

### C. Threat Model

Our threat model includes a defender, known as the model provider, and an adversary who controls a malicious user. The adversary’s goal is to steal the model and claim ownership. We assume the adversary can fine-tune the model using PEFT attacks like LoRA [24] to evade detection. The defender, with access to their own model’s parameters and the last linear layer as a fingerprint, aims to verify ownership through API access to the suspect model.

## III. LLM FINGERPRINT

### A. LLM Outputs Span A Vector Space

The transformer architecture has already become the base of numerous models due to its exceptional performance across a variety of tasks. LLMs are transformer-based models, with their pipeline presented in Fig. 1. The input text is tokenized and converted into word embeddings  $\mathbf{e}$ , with the embedding layer represented as a matrix of size  $|\mathcal{V}| \times h$ , where  $|\mathcal{V}|$  is the vocabulary size and  $h$  is the hidden size. The vocabulary size is significantly larger than the hidden size. The embeddings are processed by the transformer block with multiple layers, each containing a multi-head self-attention mechanism and a feed-forward layer, to calculate the intrinsic representation of the input and produce the intermediate representation  $\mathbf{z}$ . The last linear layer maps  $\mathbf{z}$  to logits  $\mathbf{s} \in \mathbb{R}^{|\mathcal{V}|}$ . The output of LLMs is generated by sampling from the logits  $\mathbf{s}$ . For clarity, this analysis excludes Layer Normalization [27] and RMS Normalization [28], as they primarily introduce additional multiplication terms, which do not affect the conclusions.

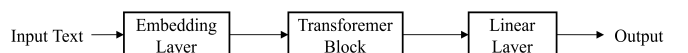


Fig. 1. The illustration of the LLMs pipeline.

It is worth noting that the logits  $\mathbf{s} = \mathbf{W}\mathbf{z}$ , where  $\mathbf{W} \in \mathbb{R}^{|\mathcal{V}| \times h}$  is the weight matrix of the last linear layer and the rank of  $\mathbf{W}$  is at most  $h$ . Every output produced by  $\mathbf{W}$  is corresponding to a vector  $\mathbf{s}$  that will always lie within a subspace of  $\mathbb{R}^{|\mathcal{V}|}$ , spanned by the columns of  $\mathbf{W}$ , which is at most  $h$ -dimensional. All possible outputs of the LLM logits will span a vector space  $\mathcal{L}$  isomorphic to the space spanned by the columns of  $\mathbf{W}$ , since they have the same dimensionality. Consequently, each LLM is associated with a distinctive vector space  $\mathcal{L}$ . This uniqueness arises because the vector space  $\mathbb{R}^{|\mathcal{V}|}$  encompasses an exceedingly large number of potential subspaces for any subspace of dimension  $h$ . For example, in the case of Gemma [3], with  $h = 2048$  and  $|\mathcal{V}| = 256000$ , the number of subspaces is extremely large. Due to variations in training initialization, datasets, configurations and hardware, it is impossible for two different LLMs to cover the same vector space. This property allows us to use it as a fingerprint for LLMs and identify their ownership. The model providers only need to retain the parameters of the last linear layer in the model. Accessing the API of the suspected model enables them to retrieve the logits, thereby verifying the ownership.

### B. Vector Space Reconstruction via API

We already demonstrated that the logits outputs from LLMs span a vector space denoted as  $\mathcal{L}$ , which we then utilized as the fingerprint. Obtaining the full logits of a model is not always feasible, as attackers aim to disclose minimal information to evade detection by the victim. In this section, we investigate a practical scenario in which our approach reconstructs the vector space for fingerprint verification and only relies on API access, enabling the retrieval of complete vocabulary probabilities, top- $k$  probabilities, or the top-1 probability.

1) *Complete probabilities of the vocabulary:* The API provides the complete probabilities  $p$  over the vocabulary. Probabilities  $\mathbf{p} = \text{softmax}(\mathbf{s})$ , all the elements of which are non-negative and have a sum that is equal to 1. It means that  $\mathbf{p}$  is a point in the simplex  $\Delta^{|\mathcal{V}|-1}$ , which lies within a  $|\mathcal{V}| - 1$  dimensional subspace of  $\mathbb{R}^{|\mathcal{V}|}$ . Additionally,  $\mathbf{p}$  is also constrained by  $\mathbf{s}$ . Due to normalization, the softmax function does not have a well-defined inverse transformation. However, if we omit it temporarily, and use the CLR (centered log-ratio) transformation, we can obtain  $\mathbf{p}'$  that differs from the original  $\mathbf{p}$  by a constant bias. From the perspective of spatial dimensions, this will introduce a one-dimensional deviation. We can manually do one-dimensional correction and will not affect the results, as  $h$  and  $|\mathcal{V}|$  are both significantly greater than 1. Therefore, we directly reconstruct the vector space  $\mathcal{P}'$  spanned by  $\mathbf{p}'$ . The value of  $\mathbf{p}'$  is computed using Equation (1), where  $g(\cdot)$  represents the geometric mean of the input.

$$\mathbf{p}' = \text{CLR}(\mathbf{p}) = \log \left( \frac{\mathbf{p}}{g(\mathbf{p})} \right) \quad (1)$$

2) *Top- $k$  probabilities:* The API provides the top- $k$  probabilities, which are the  $k$  largest elements of  $\mathbf{p}$ . In this scenario, we assume that the provider allows the user to alter token probabilities using logit bias through the API. This is

reasonable and commonly in practice. For example, OpenAI includes it in their API<sup>1</sup>. The bias is added to the specific logits of the tokens before the softmax operation, the API returns the top- $k$  probabilities. Without loss of generality, we assume that  $1, 2, \dots, m$  is the indices of the selected tokens, and the biased probabilities distribution  $\mathbf{p}^b$  is calculated by Equation (2).

$$\mathbf{p}^b = \text{softmax}(\mathbf{s}^b), \text{ where } s_i^b = \begin{cases} s_i + b & i \in \{1, \dots, m\} \\ s_i & \text{otherwise} \end{cases} \quad (2)$$

To address this scenario, we propose a method to recover the complete probabilities  $\mathbf{p}$ . For a given prompt to the model, we can obtain the top- $k$  probabilities. Suppose the reference token has the highest probability without bias, denoted as the reference probability  $p_{\text{ref}}$ . We then add a large bias  $b$  to the other  $k - 1$  tokens, pushing them into the top- $k$ . This gives us the biased probabilities  $p_i^b$  for the  $k - 1$  tokens and the biased probability  $p_{\text{ref}}^b$  for the reference token. Finally, we can calculate the unbiased probabilities  $p_i$  for the  $k - 1$  tokens using Equation (3). Complete probabilities  $\mathbf{p}$  can be obtained by querying the model with the same prompt and adding the bias  $b$  to all tokens in the vocabulary.

$$p_i = \frac{p_i^b}{p_{\text{ref}}^b} \times p_{\text{ref}} \quad (3)$$

3) *Top-1 probability:* The API yields the highest probability for a single output, akin to the top- $k$  probabilities, with  $k$  specifically set to 1. In this scenario, we present a method to recover the complete probabilities  $p$ . Suppose we introduce a substantial bias  $b$  to token  $i$ , thereby elevating it to the top position, resulting in the biased probability  $p_i^b$ . We can calculate the unbiased probability  $p_i$  for token  $i$  using Equation (4). Then, we can obtain the complete probabilities  $\mathbf{p}$  by querying the model with the same prompt and adding the bias  $b$  to all tokens in the vocabulary.

$$p_i = \frac{1}{e^{b - \log p_i^b} - e^b + 1} \quad (4)$$

It is noteworthy that theoretically, this method can potentially recover the unbiased probability in the top- $k$  scenario, albeit demanding a significantly higher number of queries. However, practical application is impeded by the presence of exponential operations, which may induce numerical instability, consequently impacting subsequent results. In contrast, the method outlined in Section III-B2 solely involves proportional operations, thus significantly mitigating issues stemming from numerical instability.

## IV. OWNERSHIP VERIFICATION

### A. Overview

The framework of ownership verification is illustrated in Fig. 2. We propose two distinct methods to verify the ownership of LLMs. The first method involves verifying whether the

<sup>1</sup><https://help.openai.com/en/articles/5247780-using-logit-bias-to-alter-token-probability-with-the-openai-api>

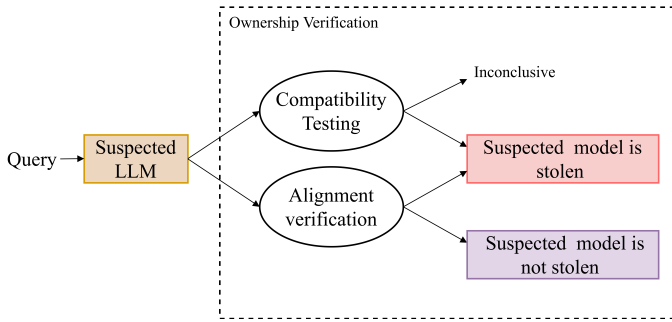


Fig. 2. The framework of ownership verification.

outputs of the suspected model occupy the same space as those of the victim model. This means that the suspected model and the victim model share the same last linear layer, facilitating the rapid identification of model infringement. Once the model has been fine-tuned, indicating that the parameters of the last linear layer have been altered, i.e., changes occur in the vector space, making verification impossible. Therefore, we introduce an alignment verification method to resolve this challenge. This method calculates the joint space dimension formed by the output vector space of the suspected model and the parameter space of the victim model. Infringement is determined by comparing the similarity of these two spaces.

### B. Compatibility Testing

As demonstrated in Section III-A, the outputs of LLMs span a vector space  $\mathcal{L}$  isomorphic to the space spanned by the columns of the last linear layer  $\mathbf{W}$ . To simplify the expression, we slightly abuse the notation by using  $\mathcal{L}$  to represent the space by the columns of the last linear layer  $\mathbf{W}$  in the following discussion. We retain the last linear layer of LLMs as private, serving as the fingerprint of the victim model. The suspected model is queried through the API to obtain its logits output  $\mathbf{s}$ . For a suspected model which is stolen from the victim model and the last linear layer does alter, the output  $\mathbf{s}$  will lie within the vector space  $\mathcal{L}$ . We can verify this by solving equation  $\mathbf{W}\mathbf{x} = \mathbf{s}$  to determine whether  $\mathbf{s}$  lies within the space  $\mathcal{L}$ . If the equation has a solution, the suspected model is considered to be derived from the victim model. However, due to numerical instability introduced by floating-point calculations, we instead calculate the Euclidean distance  $d$  between  $\mathbf{s}$  and the space  $\mathcal{L}$  to determine whether the suspected model is derived from the victim model. The  $d$  is calculated by Equation (5), where  $\hat{\mathbf{x}}$  is the solution of the equation  $\mathbf{W}\mathbf{x} = \mathbf{s}$ .

$$d = \|\mathbf{s} - \mathbf{W}\hat{\mathbf{x}}\| \quad (5)$$

We set an error term  $e$  to represent the error introduced by the numerical instability. If  $d < e$ , this implies that  $\mathbf{s}$  is compatible with the space  $\mathcal{L}$ , suggesting that the suspected model is derived from the victim model. If we only have access to probabilities  $\mathbf{p}$  and recover  $\mathbf{p}'$  using the method described in Section III-B, we manually correct the one-dimensional

deviation by appending a constant column vector to  $\mathbf{W}$  and obtain  $\mathbf{W}'$  as shown in Equation (6).

$$\mathbf{W}' = [\mathbf{W}, \mathbf{1}] \quad (6)$$

We then use  $\mathbf{W}'$  instead of  $\mathbf{W}$  to verify the ownership using the same method described above.

### C. Alignment Verification

In PEFT attacks, the suspect model has undergone fine-tuning, altered its last linear layer. The attack changes the victim model's vector space  $\mathcal{L}$ , preventing ownership verification by the method described in Section IV-B. As in manifold hypothesis, high-dimensional data can be compressed into a low-dimensional latent space, and different tasks are governed by distinct features in that space. Therefore, when fine-tuning for a specific task, it is assumed to impact only a portion of the space  $\mathcal{L}$ , not the entire space. Especially, in PEFT attacks like LoRA, the model is fine-tuned with a low-rank matrix. The parameters are updated by  $\mathbf{W}_N = \mathbf{W}_O + \Delta\mathbf{W}$ , where  $\Delta\mathbf{W}$  is a matrix which rank is no more than  $k$ . If there is substantial overlap between the output space  $\mathcal{L}$  of the suspect model and the space spanned by the columns of the victim model  $\mathbf{W}$ , it indicates that the suspect model closely resembles the victim model and may have been derived through unauthorized replication.

In practice, we calculate the dimension formed by the union of the output vector space of the suspect model and the parameter space of the victim model, denoted as  $\mathcal{L}_{\text{sum}}$ . If the dimension of  $\mathcal{L}_{\text{sum}}$  is close to that of  $\mathcal{L}$ , it indicates that the suspect model is derived from the victim model. Otherwise, it is not. For matrices containing numerous floating-point numbers, directly calculating the rank is not advisable, as it can lead to significant errors due to numerical inaccuracies. Instead, we introduce **Algorithm 1** to calculate the dimension difference  $\Delta r$  between  $\mathcal{L}_{\text{sum}}$  and  $\mathcal{L}$ .

Once  $\Delta r$  is obtained, it can be used to determine if the suspect model is derived from the victim model. If  $\Delta r$  is much less than an order of magnitude compared to the hidden size  $h$ , which indicates that the suspect model is indeed derived from the victim model. In probabilities access scenarios,  $\Delta r$  will only experience a numerical disturbance of one, which will not affect our results.

## V. EXPERIMENT RESULTS AND ANALYSIS

### A. Experimental Setup

We employed Gemma [3] with a hidden size of 2048 as the victim model and fine-tuned it by LoRA [24] as attack method. The LoRA [24] module was applied to the query, key and value module in attention mechanism [18] or the linear module in the last layer. The ranks of LoRA [24] were set to 16, 32 and 64. The models were fine-tuned on the Alpaca dataset [29] and the SAMSum dataset [30] to simulate different scenarios. Additionally, we also compared with a new version termed as Gemma-2, which shares the same structure but under a novel training method, leading to substantial income and completely different outputs for the identical inputs.

**Algorithm 1** Pseudocode for dimension difference calculation

**Input:**  $\mathbf{W}$ : the parameter matrix of the last linear layer in the victim model;  $\mathcal{M}$ : the suspected model;  $\mathcal{Q}$ : the query set;  $N$ : the least number of samples;  $e$ : the error term.

**Output:**  $\Delta r$ : the dimension difference.

```

1: Initialize  $\Delta r = 0, n = 0, \mathcal{S} = \emptyset$ .
2: while  $n \leq N$  do
3:   Randomly sample a query  $q$  from  $\mathcal{Q}$ 
4:   Get the logits outputs  $\mathcal{O} = \{s_1, s_2, \dots\}$  by querying the suspected model  $\mathcal{M}$  with  $q$ 
5:    $\mathcal{S} \leftarrow \mathcal{S} \cup \mathcal{O}$ 
6:    $n = \text{size}(\mathcal{S})$ 
7: end while
8: for  $i = 1, 2, \dots, n$  do
9:   Solve  $\mathbf{W}\mathbf{x}_i = \mathbf{s}_i$  to obtain  $\hat{\mathbf{x}}_i$ 
10:  Call Eq. (5) to determine  $d_i$ 
11:  if  $d_i > e$  then
12:     $\Delta r = \Delta r + 1$ 
13:  end if
14: end for
15: return  $\Delta r$ 

```

TABLE I  
COMPATIBILITY TESTING RESULTS ON VARIOUS MODEL VERSIONS AND MODELS FINE-TUNED WITH DIFFERENT MODULES AND RANKS.

	full logits	full probabilities	top-5 probabilities	top-1 probability
Gemma	$8.0 \times 10^{-5}$	$3.4 \times 10^{-3}$	$3.4 \times 10^{-3}$	$8.3 \times 10^{-5}$
Gemma-2	$5.5 \times 10^5$	$5.5 \times 10^5$	$5.5 \times 10^5$	$5.5 \times 10^5$
SAMSum				
qkv-16	$9.7 \times 10^{-5}$	$1.4 \times 10^{-4}$	$1.4 \times 10^{-4}$	$1.0 \times 10^{-4}$
qkv-32	$8.5 \times 10^{-5}$	$3.6 \times 10^{-3}$	$3.6 \times 10^{-3}$	$9.6 \times 10^{-5}$
qkv-64	$1.1 \times 10^{-4}$	$9.5 \times 10^{-4}$	$9.5 \times 10^{-4}$	$9.9 \times 10^{-5}$
linear-16	$7.3 \times 10^5$	$7.2 \times 10^5$	$7.2 \times 10^5$	$7.2 \times 10^5$
linear-32	$6.9 \times 10^5$	$6.8 \times 10^5$	$6.8 \times 10^5$	$6.9 \times 10^5$
linear-64	$7.6 \times 10^5$	$7.5 \times 10^5$	$7.5 \times 10^5$	$7.5 \times 10^5$
Alpaca				
qkv-16	$8.3 \times 10^{-5}$	$5.7 \times 10^{-4}$	$5.7 \times 10^{-4}$	$8.4 \times 10^{-4}$
qkv-32	$7.0 \times 10^{-5}$	$2.8 \times 10^{-3}$	$2.8 \times 10^{-3}$	$8.5 \times 10^{-5}$
qkv-64	$6.8 \times 10^{-5}$	$1.6 \times 10^{-4}$	$1.6 \times 10^{-4}$	$8.1 \times 10^{-5}$
linear-16	$6.8 \times 10^5$	$6.7 \times 10^5$	$6.7 \times 10^5$	$6.7 \times 10^5$
linear-32	$6.7 \times 10^5$	$6.6 \times 10^5$	$6.6 \times 10^5$	$6.6 \times 10^5$
linear-64	$6.9 \times 10^5$	$6.8 \times 10^5$	$6.8 \times 10^5$	$6.9 \times 10^5$

### B. Compatibility Testing Results

In the compatibility testing, we assume that malicious users might release their stolen model either in its original form or after fine-tuning it. Fine-tuning is on the attention mechanism in the intermediate layers or the last linear layer. We generated (or recovered) 300 complete logits (or probabilities) through random queries and calculated the average Euclidean distance  $d$ . We retained the parameters of Gemma’s last linear layer and conducted verification experiments across various models. The results of the compatibility testing method are presented in

TABLE II  
DIMENSION DIFFERENCE RESULTS ON VARIOUS MODEL VERSIONS AND MODELS FINE-TUNED WITH DIFFERENT MODULES AND RANKS.

	full probabilities	top-5 probabilities	top-1 probability
Gemma	1	1	1
Gemma-2	300	300	300
SAMSum			
qkv-16	1	1	1
qkv-32	1	1	1
qkv-64	1	1	1
linear-16	11	11	11
linear-32	12	12	11
linear-64	11	11	11
Alpaca			
qkv-16	1	1	1
qkv-32	1	1	1
qkv-64	1	1	1
linear-16	16	16	16
linear-32	21	21	20
linear-64	22	22	21

Table I. Each column corresponds to the results of  $d$  under different API scenarios, while each row represents the outcomes for different models. In the table, ‘qkv’ and ‘linear’ represent LoRA module was applied to the query, key and value module in the attention mechanism or the linear module in the last layer, respectively, with their suffixes indicating the rank of LoRA. The experimental results clearly reveal that for models fine-tuned on the last layer or not, a significant difference exists between them and other models. This distinction is adequate for ascertaining ownership, verifying the effectiveness of the proposed method. It is worth to note that although this is the average results, this consistency will hold even with only a few samples in practice, thus also enabling rapid verification.

### C. Alignment Verification Results

To minimize computational and time overhead, the value of  $N$  was set to 300 in **Algorithm 1**, considering that the value of  $\Delta r$  is strictly constrained under the PEFT attacks. We obtained 300 complete probabilities through random queries and calculated results of  $\Delta r$  to evaluate the effectiveness of the alignment verification method. We preserved the parameters of Gemma’s last linear layer and conducted  $\Delta r$  across various models. Table II presents the results of the dimension difference calculation. Each row depicts the results of  $\Delta r$  with different models using **Algorithm 1**, while each column shows the outcomes across various API scenarios. The configuration of PEFT attacks is the same as that in Section V-B. In the table, ‘qkv’ and ‘linear’ respectively denote LoRA module was applied to the query, key and value module in the attention mechanism or the linear module in the last layer, with their suffixes indicating the rank of LoRA. We observe that the  $\Delta r$  value of the Gemma and the model fine-tuned on the intermediate layers equals 1, which is the result of the CLR transformation. For the models fine-tuned on the last layer,

the  $\Delta r$  value is close to the rank of LoRA and much less than  $h$ , providing the evidence to ascertain that the suspected model originates from the victim model. It is noteworthy that models fine-tuned on the last layer exhibit approximately equal values of  $\Delta r$  despite having a larger rank, which is consistent with the assumption of PEFT that the updated weights during model fine-tuning have a low intrinsic rank. The intrinsic rank is also influenced by the datasets and reflected in the values of  $\Delta r$ . Experiments show that the proposed method can verify the copyright, despite PEFT attacks.

Furthermore, to investigate the relationship between Gemma and Gemma-2, we obtained 3000 probability vectors of Gemma-2 and got the value of  $\Delta r$  is 2052. This result implies that the Gemma-2 has undergone extensive fine-tuning or training from scratch compared to Gemma and also confirms that the uniqueness of the proposed fingerprint. Note that the value of  $\Delta r$  is not exactly the same as  $h$  due to the accuracy of numerical calculation, but they are of the same magnitude.

## VI. CONCLUSION

In this paper, we propose a novel fingerprinting method for LLMs that is generalized and capable of verifying fingerprint in a black-box scenario without requiring model training or compromising in model functionality. Specifically, we analyze the model's outputs and present two methods for copyright verification. First, we introduce a comprehensive testing method to swiftly ascertain whether the suspect model is identical to the victim model. To address scenarios involving PEFT attacks, we also propose an alignment verification method for copyright verification. Furthermore, we develop a reconstruction method to recover the complete information under API access. Our empirical study shows that our proposed method achieves supervisor verification performance and robustness against PEFT attacks. Our proposed method also reveals inherent characteristics of LLMs and offers a promising solution for advancing ownership verification of LLMs.

## ACKNOWLEDGEMENT

This work was supported by the Natural Science Foundation of China under Grant Number U23B2023.

## REFERENCES

- [1] H. Touvron, T. Lavril, G. Izacard *et al.*, "Llama: Open and efficient foundation language models," *arXiv preprint arXiv:2302.13971*, 2023.
- [2] H. Touvron, L. Martin, K. Stone *et al.*, "Llama 2: Open foundation and fine-tuned chat models," *arXiv preprint arXiv:2307.09288*, 2023.
- [3] G. Team, T. Mesnard, C. Hardin *et al.*, "Gemma: Open models based on gemini research and technology," *arXiv preprint arXiv:2403.08295*, 2024.
- [4] A. Q. Jiang, A. Sablayrolles, A. Mensch *et al.*, "Mistral 7b," *arXiv preprint arXiv:2310.06825*, 2023.
- [5] Y. Uchida, Y. Nagai, S. Sakazawa *et al.*, "Embedding watermarks into deep neural networks," in *Proceedings of the 2017 ACM International Conference on Multimedia Retrieval*, 2017, p. 269–277.
- [6] J. Wang, H. Wu, X. Zhang *et al.*, "Watermarking in deep neural networks via error back-propagation," *Electronic Imaging*, vol. 32, pp. 1–9, 2020.

- [7] B. Darvish Rouhani, H. Chen, and F. Koushanfar, "Deepsigns: An end-to-end watermarking framework for ownership protection of deep neural networks," in *Proceedings of the Twenty-Fourth International Conference on Architectural Support for Programming Languages and Operating Systems*, 2019, p. 485–497.
- [8] P. Fernandez, G. Couairon, T. Furon *et al.*, "Functional invariants to watermark large transformers," in *IEEE International Conference on Acoustics, Speech and Signal Processing*, 2024, pp. 4815–4819.
- [9] Y. Adi, C. Baum, M. Cisse *et al.*, "Turning your weakness into a strength: Watermarking deep neural networks by backdooring," in *27th USENIX Security Symposium*, 2018, pp. 1615–1631.
- [10] X. Zhao, H. Wu, and X. Zhang, "Watermarking graph neural networks by random graphs," in *IEEE International Symposium on Digital Forensics and Security*, 2021, pp. 1–6.
- [11] Y. Liu, H. Wu, and X. Zhang, "Robust and imperceptible black-box dnn watermarking based on fourier perturbation analysis and frequency sensitivity clustering," *IEEE Transactions on Dependable and Secure Computing*, 2024.
- [12] H. Wu, G. Liu, Y. Yao, and X. Zhang, "Watermarking neural networks with watermarked images," *IEEE Transactions on Circuits and Systems for Video Technology*, vol. 31, no. 7, pp. 2591–2601, 2021.
- [13] N. Lukas and F. Kerschbaum, "PTW: Pivotal tuning watermarking for Pre-Trained image generators," in *32nd USENIX Security Symposium*, 2023, pp. 2241–2258.
- [14] P. Fernandez, G. Couairon, H. Jégou *et al.*, "The stable signature: Rooting watermarks in latent diffusion models," in *International Conference on Computer Vision*, 2023, pp. 22 409–22 420.
- [15] H. J. Song, M. Khayatkhoei, and W. AbdAlmageed, "Manifpt: Defining and analyzing fingerprints of generative models," *arXiv preprint arXiv:2402.10401*, 2024.
- [16] J. Xu, F. Wang, M. D. Ma *et al.*, "Instructional fingerprinting of large language models," *arXiv preprint arXiv:2401.12255*, 2024.
- [17] B. Zeng, C. Zhou, X. Wang *et al.*, "Huref: Human-readable fingerprint for large language models," *arXiv preprint arXiv:2312.04828*, 2023.
- [18] A. Vaswani, N. Shazeer, N. Parmar *et al.*, "Attention is all you need," in *Advances in Neural Information Processing Systems*, vol. 30, 2017.
- [19] N. Carlini, D. Paleka, K. D. Dvijotham *et al.*, "Stealing part of a production language model," *arXiv preprint arXiv:2403.06634*, 2024.
- [20] Z. Yang, Z. Dai, R. Salakhutdinov *et al.*, "Breaking the softmax bottleneck: A high-rank rnn language model," in *International Conference on Learning Representations*, 2018.
- [21] M. Finlayson, J. Hewitt, A. Koller *et al.*, "Closing the curious case of neural text degeneration," in *International Conference on Learning Representations*, 2024.
- [22] M. Finlayson, S. Swayamdipta, and X. Ren, "Logits of api-protected llms leak proprietary information," *arXiv preprint arXiv:2403.09539*, 2024.
- [23] N. Houlsby, A. Giurgiu, S. Jastrzebski *et al.*, "Parameter-efficient transfer learning for NLP," in *International Conference on Machine Learning*, vol. 97, 2019, pp. 2790–2799.
- [24] E. J. Hu, Y. Shen, P. Wallis *et al.*, "LoRA: Low-rank adaptation of large language models," in *International Conference on Learning Representations*, 2022.
- [25] T. Dettmers, A. Pagnoni, A. Holtzman *et al.*, "Qlora: Efficient finetuning of quantized llms," *Advances in Neural Information Processing Systems*, vol. 36, 2024.
- [26] F. Meng, Z. Wang, and M. Zhang, "Pissa: Principal singular values and singular vectors adaptation of large language models," *arXiv preprint arXiv:2404.02948*, 2024.
- [27] J. L. Ba, J. R. Kiros, and G. E. Hinton, "Layer normalization," *arXiv preprint arXiv:1607.06450*, 2016.
- [28] B. Zhang and R. Sennrich, "Root mean square layer normalization," in *Advances in Neural Information Processing Systems*, vol. 32, 2019.
- [29] Y. Dubois, X. Li, R. Taori *et al.*, "Alpacafarm: A simulation framework for methods that learn from human feedback," *Advances in Neural Information Processing Systems*, vol. 36, 2024.
- [30] B. Gliwa, I. Mochol, M. Biesek *et al.*, "SAMSum corpus: A human-annotated dialogue dataset for abstractive summarization," in *2nd Workshop on New Frontiers in Summarization*, 2019, pp. 70–79.